

# Certain aspects of Green element computational model for BOD–DO interaction

Okey Oseloka Onyejekwe\*, Shaileen Toolsi

*Faculty of Engineering, University of Durban-Westville, Private Bag X54001, Durban 4000, South Africa*

Received 3 January 2000; received in revised form 26 July 2000; accepted 7 August 2000

## Abstract

The physical laws governing the interaction of biochemical oxygen demand (BOD), and dissolved oxygen (DO) in a water body are expressed as coupled one-dimensional, transient partial differential equations and solved by the Green element method (GEM). The GEM has been developed as a flexible, hybrid numerical approach, that utilizes the finite element methodology to achieve optimum, inter-nodal connectivity in the problem domain, while at the same time retaining the elegant second order accurate formulation of the boundary element method (BEM). While overcoming some of the limitations of classical boundary element approach, GEM guarantees a sparsely populated coefficient matrix, which is easy to handle numerically. We test the reliability of GEM by solving a one-dimensional mass transport model that simulates BOD–DO dynamics in a stream. The results compare favorably with those obtained analytically, and by the finite element method (FEM) Galerkin procedure. © 2000 Elsevier Science Ltd. All rights reserved.

*Keywords:* Green element method; Finite element method; BOD–DO dynamics

## 1. Introduction

As the environment becomes further degraded because of pollution arising from industrial and commercial activities, a lot of interest is being devoted to the solution of mass transport equations. As most of these equations are too complex to be solved analytically, mathematical models have been used as predictive tools in evaluating the causes of pollution, and possible cures. The rapid advance of the science and art of mathematical modelling, has led to the development of more comprehensive and sophisticated numerical models for the study of environmental pollution. Yet, many of these attempts are still either of a preliminary nature or not sufficiently comprehensive. In some simulations, some of the factors that influence mass transport are totally omitted, while in others essential phenomena are lumped together and represented by a simplified mathematical relationship.

Following the work of Guymon [1], Price et al. [2], a lot of effort has been devoted to the numerical solution

of the convection–dispersion equation (C–D equation). This interest has been sustained by the advantage of applying one-dimensional C–D equation to study mass transfer in natural aquatic systems. In comparison to their multi-dimensional counterparts, one-dimensional C–D equations have an obvious advantage of mathematical tractability. In addition, they can be used to supply information that is related to accessible or observational field data. This is especially true when modelling mass transfer equations for water quality parameters involving source and sink terms, such as BOD and DO.

One of the earliest attempts to numerically solve the C–D equation, was done with the finite difference technique (Price et al. [2], Book et al. [3]). Tucci and Chen [4] later used finite difference techniques to solve BOD–DO dynamics in an aquatic system. The finite element method (FEM) was later introduced as an alternative to deal with the spatial independent variable in the C–D equation, while the time was left to the conventional finite difference technique (Gray and Pinder [5]). The work by Taigbenu and Liggett [6] should rank as one of earliest efforts to solve the C–D equation with the boundary element method (BEM). Subsequent work to improve on the performance of the BEM can be found

\* Corresponding author. Tel.: +27-31-204-4749; fax: +27-31-204-4291.

*E-mail address:* okey@pixie.udw.ac.za (O.O. Onyejekwe).

in Cheng [7] and Brebbia et al. [8]. In a later attempt to overcome some of the deficiencies of the BEM, Taigbenu and Onyejekwe [9] applied the Green element method (GEM) to solve the C–D equation, and came up with very accurate results even for high Peclet numbers.

The relative success registered by the FEM in the solution of the C–D equation, is often times attributed to its formulation robustness, which ensures inter-nodal connectivity, and species transport along the nodal links in any direction. The GEM not only acquires this advantage because of its hybrid formulation, in addition, it is also able to handle infinite domain, point and distributed sources in a manner that is typical of the BEM.

In the work reported herein, the GEM is used to solve BOD–DO coupled mass transport problem involving such key features as: (i) axial convective transport of mass; (ii) axial dispersion of mass; (iii) interaction between BOD and DO; (iv) re-aeration and decay.

GEM numerical results are then compared with those obtained analytically, and with the Galerkin FEM.

## 2. Governing equations

The BOD–DO dynamics in a stream is described by a set of coupled one-dimensional C–D equations, and considers the effects of: (i) advection; (ii) dispersion; (iii) internal sources and sinks including point and non-point sources of pollution. These equations are given by

$$\frac{\partial B}{\partial t} + \frac{\partial(UB)}{\partial x} = \frac{\partial}{\partial x} \left( E_B \frac{\partial B}{\partial x} \right) - K_B B + L_B + \sum_{j=1}^{N_p} \frac{Q_j B_j}{A_j} \delta(x - x_j), \quad (1a)$$

$$\frac{\partial DO}{\partial t} + \frac{\partial(UDO)}{\partial x} = \frac{\partial}{\partial x} \left( E_D \frac{\partial DO}{\partial x} \right) - K_D B + R_D + K_R (DO^{\text{SAT}} - DO) + \sum_{j=1}^{N_p} \frac{Q_j DO_j}{A_j} \delta(x - x_j), \quad (1b)$$

where  $B$  is the BOD concentration,  $DO$  the DO concentration,  $DO^{\text{SAT}}$  the saturation DO concentration,  $E_B$  the BOD dispersion coefficient,  $E_D$  the DO dispersion coefficient,  $K_B$  the BOD decay rate,  $K_D$  the BOD deoxygenation rate,  $L_B$  the BOD distributed source,  $K_R$  the re-aeration rate,  $R_D$  the DO distributed source,  $Q_j$  the volumetric flow rate of load at point  $j$ ,  $B_j$  the BOD concentration at point  $j$ ,  $DO_j$  the DO concentration at point  $j$ ,  $A_j$  the cross-sectional area of stream at point of load discharge, and  $N_p$  is the number of point loads.

Eqs. (1a) and (1b) come from averaging of the point C–D equation over the stream cross-sectional area.

## 3. Green element formulations

The GEM implementation of governing equations is motivated by a hybrid BEM–FEM procedure, which basically consists of a BEM formulation and a FEM implementation. Details of this procedure have earlier been reported in Taigbenu and Onyejekwe [9] and Onyejekwe [10]. However, for the sake of clarity, we shall give a brief and axiomatic account of certain aspects of GEM formulation that pertain to this problem. We start by obtaining the integral replication of the governing partial differential equations (since the same steps apply to both Eqs. (1a) and (1b), we shall concentrate on only one of the equations). This is achieved by utilizing a suitable complementary equation of the differential operator and its fundamental solution. These are given by

$$\frac{d^2 G}{dx^2} = \delta(x - x_i) \quad -\infty \leq x \leq \infty, \quad (2a)$$

$$G(x, x_i) = \frac{|x - x_i| + k}{2}, \quad (2b)$$

where  $x_i$  identifies the position of the source node,  $k$  is an arbitrary constant, whose value is chosen so that GEM should always provide physically meaningful results. For example  $k$  should never be zero because it results in a singular matrix for the flux terms. We have therefore judiciously set  $k$  as the longest spatial element in the problem domain. The *Dirac delta* ( $\delta(x - x_i)$ ) forcing function or the response function of the problem statement originates from the boundary integral theory and guarantees the scheme's second order accuracy over an infinite domain.

The key to achieve an integral replication of the governing partial differential equation lies in the *Green's second identity*. Within a generic element  $[x_1^{(e)}, x_2^{(e)}]$ , the integral equation becomes

$$\int_{x_1^{(e)}}^{x_2^{(e)}} \left[ B \delta(x - x_i) - G \left( U \varphi(x, t) + \frac{\partial B}{\partial t} + K_B B - L_B - f_j \right) \right] dx = B \frac{dG}{dx} \Big|_{x_1^{(e)}}^{x_2^{(e)}} - G \frac{dB}{dx} \Big|_{x_1^{(e)}}^{x_2^{(e)}}, \quad (2c)$$

substituting Eqs. (2a) and (2b) into Eq. (2c) yields

$$\begin{aligned} E_B \left[ -\lambda_i^{(e)} B^{(e)}(x_i, t) + G^*(x_2^{(e)}, x_i^{(e)}) B^{(e)}(x_2^{(e)}, t) \right. \\ \left. - G^*(x_1^{(e)}, x_i^{(e)}) B^{(e)}(x_1^{(e)}, t) - G(x_2^{(e)}, x_i^{(e)}) \varphi(x_2^{(e)}, t) \right. \\ \left. + G(x_1^{(e)}, x_i^{(e)}) \varphi(x_1^{(e)}, t) \right] \int_{x_1^{(e)}}^{x_2^{(e)}} G(x^{(e)}, x_i^{(e)}) \\ \times \left[ U \varphi(x^{(e)}, t) + \frac{\partial B^{(e)}}{\partial t} + K_B B^{(e)} - L_B - f_j^{(e)} \right] \\ dx = 0, \quad i = 1, 2, \end{aligned} \quad (3a)$$

where  $e$  refers to a typical element of the problem domain.  $f_j$  represents point or distributed source, and  $\varphi$  represents the spatial differentiation of the dependent variable.  $\lambda$  is a parameter, which takes into account the location of the source point within an element. It makes use of the properties of the dirac delta function.  $\lambda = 1$  when  $x_i$  is within the problem domain  $[x_1, x_2]$  and  $\lambda = 0.5$  when  $x_i$  is located at the end points of  $x_1$  and  $x_2$ .

$$\frac{dG}{dx} = G^* = \frac{1}{2} [H(x - x_i) - H(x_i - x)], \quad (3b)$$

where  $H(x - x_i)$  is the Heaviside function. Eqs. (3a) and (3b), the so called *weak statement* of the governing partial differential equation belongs to the *Fredholm integral equation of the second kind*. Up to this level of formulation, the GEM is identical to BEM. We further observe that the absence of any form of a *residual* or any overt attempt to minimize it implies that no approximation has so far been introduced. It is this accurate and elegant formulation that contributes to both the BEM and Green element second order convergence.

GEMs hybrid approach starts with the solution of Eq. (3a) on each element of the problem domain. With this step, the evolution of BEM from a technique limited to the boundaries of the problem domain to a more general method that deals with both the domain and the boundaries along the lines of boundary integral theory is guaranteed. In order to evaluate the line integral over an element, the dependent variables are interpolated in line with a typical finite element procedure. For example using linear element shape functions, both the primary dependent variable, and its spatial derivative are given by

$$\begin{aligned} B(x, t) &\approx \Omega_1(\zeta)B_1(t) + \Omega_2(\zeta)B_2(t), \\ \varphi(x, t) &\approx \Omega_1(\zeta)\varphi_1(t) + \Omega_2(\zeta)\varphi_2(t), \end{aligned} \quad (4)$$

where  $\Omega_1$  and  $\Omega_2$  are linear shape functions and are represented as

$$\Omega_1 = 1 - \zeta, \quad \Omega_2 = \zeta. \quad (5)$$

Eq. (4) guarantees that dependent variables are represented within each element by using interpolation functions to describe the variables in terms of nodal unknowns. We mention in passing that it is only at this stage, that any approximation is introduced into GEM formulation. So far the process of converting the governing differential equation into its integral form has involved a response function and not a residual to be minimized.

Solution of the integral equation on the elements of the problem domain results in a set of equations for each element in which there are as many equations as there are nodal unknowns. This set of equations are then assembled to give a set of global equations in which the unknowns are the nodal values of each dependent variable. Eq. (3a) can therefore be expressed as a sum-

mation of the integral contribution from each element, and is given as

$$\begin{aligned} \sum_{e=1}^M E_B &\left[ -\lambda_i^{(e)} B^{(e)}(x_i, t) + G^* \left( x_2^{(e)}, x_i^{(e)} \right) B^{(e)} \left( x_2^{(e)}, t \right) \right. \\ &- G^* \left( x_1^{(e)}, x_i^{(e)} \right) B^{(e)} \left( x_1^{(e)}, t \right) \\ &- G \left( x_2^{(e)}, x_i^{(e)} \right) \varphi \left( x_2^{(e)}, t \right) + G \left( x_2^{(e)}, x_i^{(e)} \right) \varphi \left( x_1^{(e)}, t \right) \left. \right] \\ &+ \int_{x_1^{(e)}}^{x_2^{(e)}} G \left( x^{(e)}, x_i^{(e)} \right) \left[ U \varphi \left( x^{(e)}, t \right) + \frac{\partial B^{(e)}}{\partial t} + K_B B^{(e)} \right. \\ &\left. - L_B - f_j^{(e)} \right] dx = 0, \quad i = 1, 2, \end{aligned} \quad (6)$$

where  $M$  is the number of elements in the problem domain. The time derivative in Eq. (6) can be handled by a finite difference approximation

$$\begin{aligned} \frac{dB_j}{dt} \Big|_{t=t_m+\alpha\Delta t} &\approx \frac{B_j(t_m + \Delta t) - B_j(t_m)}{\Delta t} \\ &= \frac{B_j^{m+1} - B_j^m}{\Delta t}, \quad 0 \leq \alpha \leq 1, \end{aligned} \quad (7)$$

where  $m + 1$ ,  $m$  represents the current and previous times, respectively. Substituting Eq. (7) into Eq. (6), the element discrete equation for a two-level time scheme is given as

$$\begin{aligned} &\left[ \alpha (E_B R_{ij} + (K_B - L_B) T_{ij}) + \frac{T_{ij}}{\Delta t} \right] B_j^{m+1} + \alpha [(E_B L_{ij} \\ &+ U T_{ij})] \varphi_j^{m+1} \left[ (1 - \alpha) (E_B R_{ij} + (K_B - L_B) T_{ij}) + \frac{T_{ij}}{\Delta t} \right] B_j^m \\ &+ (1 - \alpha) [(E_B L_{ij} + U T_{ij})] \varphi_j^m T_{ij} \\ &\times \left[ (\alpha) f_j^{(m+1)} + (1 - \alpha) f_j^{(m+1)} \right] = 0, \\ &i, j = 1, 2, \quad 0 \leq \alpha \leq 1, \end{aligned} \quad (8)$$

where the coefficient matrices  $L_{ij}$ ,  $T_{ij}$ , and  $R_{ij}$  are the same as specified in Taigbenu and Onyejekwe [9], Onyejekwe [10].

Many water quality problems deal with an ingress of contaminated discharge form a point source into a water body. This can either occur as an accidental spillage, leakage, or as an effluent discharge from an industry. Given the overall effect of such an occurrence on water quality, it is necessary that reliable methods be developed to quantify the level of contamination. We therefore turn out attention to point or concentrated sources or sinks and demonstrate how they can be efficiently handled by the Green element numerical technique.

We note that in Eqs. (1a) and (1b) that the recharge contains both point and distributed components, and can be represented by

$$f_j = f_{pj} + f_{dj}. \quad (9)$$

The point source in Eq. (9) can be written as

$$f_{p_j} = \sum_{j=1}^{N_p} Z_j \delta(x - x_j), \quad (10a)$$

where  $Z_j$  is the strength of the  $j$ th source or sink located at  $x_j$ . Inserting Eq. (10a) into the line integral of Eq. (3a) we obtain

$$\begin{aligned} F_1^{(e)} &= \int_{x_1^{(e)}}^{x_2^{(e)}} \frac{1}{E_B} \sum_{j=1}^{N_p^{(e)}} Z_j \delta(x - x_j) (x - x_1^{(e)} + k) dx \\ &= \frac{1}{E_B} \sum_{j=1}^{N_p^{(e)}} Z_j (x_j - x_1^{(e)} + k), \end{aligned} \quad (10b)$$

when the source node is at  $x_1$ . The integral value when the source node is at  $x_2$  is

$$\begin{aligned} F_2^{(e)} &= \int_{x_1^{(e)}}^{x_2^{(e)}} \frac{1}{E_B} \sum_{j=1}^{N_p^{(e)}} Z_j \delta(x - x_j) (x_2^{(e)} - x + k) dx \\ &= \frac{1}{E_B} \sum_{j=1}^{N_p^{(e)}} Z_j (x_2^{(e)} - x_j + k) \end{aligned} \quad (10c)$$

The distributed sources are handled more straightforwardly. Following the same steps as above, their values at the nodes of an element  $[x_1, x_2]$  are

$$F_1 = \int_{x_1}^{x_2} f_{d_j} (x - x_1 + k) dx, \quad (10d)$$

$$F_2 = \int_{x_1}^{x_2} f_{d_j} (x_2 - x + k) dx, \quad (10e)$$

Using the Gaussian quadrature technique, Eqs. (10d) and (10e) are evaluated as

$$F_1^{(e)} = \frac{l^{(e)}}{2E_B} \sum_{r=1}^{N_d^{(e)}} w_r f(x_r) (x_r - x_1^{(e)} + k) \quad (10f)$$

and

$$F_2^{(e)} = \frac{l^{(e)}}{2E_B} \sum_{r=1}^{N_d^{(e)}} w_r f(x_r) (x_2^{(e)} - x_r + k), \quad (10g)$$

where  $N_d$  is the number of distributed sources or sinks,  $l^{(e)}$  is the length of an element.

GEMs hybrid formulation facilitates the analytical implementation of all the terms within the integral sign of Eq. (3a) as well as the coefficient matrices of Eq. (8). This advantage is principally due to the fact that both the field and the source nodes are always situated within the same element. On the contrary, BEM technique requires that the line integral be split into two parts in order to take care of the discontinuity resulting from both the dirac delta and the Heaviside functions at the source node. Integration is no longer straightforward as the resulting singularity oftentimes demands rigorous or ad-hoc integration procedures. The level of rigor thus introduced

even for relatively simple problems has limited the scope of BEM application, especially for those problems, where the problem domain must be encountered.

#### 4. Finite element approach

We observe that the governing equations are not self-adjoint, and hence cannot be solved by the minimization of variational forms. Therefore, we cannot apply the numerical machinery associated with the Ritz method. This has prompted the use of the finite element Galerkin's technique based on the method of weighted residual. Invoking the Green's theorem, and applying the Galerkin's technique, we can divide Eq. (1a) into segments over the whole problem domain. If the total number of segments is  $M$ , then the resulting residual  $R_i$  is given by

$$\begin{aligned} R_i &= \sum_{m=1}^M \left[ \int_{x_m^-}^{x_m^+} E_B \frac{\partial^2 DO}{\partial x^2} - U \frac{\partial DO}{\partial x} - K_B DO + L_B - \frac{\partial DO}{\partial t} \right] \\ &\quad + \sum_{j=1}^N \left[ \int_{x_j^-}^{x_j^+} E_B \left( \frac{\partial^2 DO}{\partial x^2} \right) DO_i(x) dx + \frac{Q_i DO_i}{A_i} \right], \end{aligned} \quad (11)$$

where  $N$  is the node at the end of an element. Details of how to proceed from Eqs. (13a)–(13c) can be found in standard finite element text books and are not repeated here. The final matrix equation can be written as

$$[A_{ij}] \frac{dDO_j}{dt} - [B_{ij}] DO_j + [\omega_j] = 0. \quad (12)$$

Eq. (12) is a linear, transient, Galerkin's finite element model equation, which together with the Green element model is applied to solve a BOD–DO dynamics problem.

#### 5. Model verification and discussions

##### 5.1. Case 1

In order to verify the validity and reliability of the GEM model developed herein and to compare our results with another method, we shall purposely choose a problem, which has a closed form solution. We shall consider an infinite domain  $-5 \leq x \leq 15$  km. The problem parameters are  $U = 1.0$  km/day, for BOD  $L_B = 0.5$ /day,  $K_B = 2.0$ /day,  $E_B = 1.0$  m<sup>2</sup>/day, the concentrated load for dissolved oxygen at  $x = 0.0$  is  $(Q_1 B_1 / A_1) = 1.0$  mg/m/day. For DO,  $R_D = -0.2$  mg/l/day,  $K_R = 1.5$  m/day,  $DO^{\text{SAT}} = 3.0$  mg/l, and DO concentrated load at  $x = 0$  is  $(Q_1 DO_1 / A_1) = 0.5$  mg/m/day. The initial and boundary conditions for the coupled system are

$$B(x, 0) = DO(x = -5, t) = 1.0 \text{ mg/l}, \quad (13a)$$

$$B(x = -5) = DO(x = -5) = 1.0 \text{ mg/l}, \quad (13b)$$

$$\frac{dB}{dx}(x = -15 \text{ km}) = \frac{dDO}{dx}(x = -15 \text{ km}) = 0. \quad (13c)$$

The steady-state analytical solution to this problem can be determined. It is

$$B = 0.005053 e^{-x} + \frac{1}{3} e^{2x} + 0.25, \quad -5 \text{ km} \leq x \leq 0,$$

$$B = 0.33839 e^{-x} + 0.25, \quad 0 \leq x \leq 15 \text{ km}$$

$$DO = -1.3228 e^{1.8229x} - 0.0740 e^{-0.8229x} + 1.3333 e^{2x} \quad (14)$$

$$+ 0.020212 e^{-x} + 2.533, \quad -5 \text{ km} \leq x \leq 0,$$

$$DO = -1.3968 e^{-0.8229x} + 1.3536 e^{-x}$$

$$+ 2.533, \quad 0 \leq x \leq 15 \text{ km}.$$

Both FEM and GEM numerical models are solved with 41 grid points spaced evenly until steady-state, and their results compared with the solution of Eq. (14). Eqs. (8) and (12) represent a time-marching procedure, which will generate the concentration profiles for both BOD and DO with respect to time and space. Since, BOD appears as a variable in both Eqs. (1a) and (1b), Eq. (1a) is solved first, and once  $B(x, t)$  is determined, then  $K_B B$  is fed into the computation of Eq. (1b) as a source term in order to achieve numerical coupling. Since, linear shape functions are used for the interpolation of the dependent variables, the arithmetic mean of  $B$  (BOD) is used to evaluate the DO source term, which is used in the numerical solution of Eq. (1b). The varying source term is calculated by

$$S_{DO} = -K_B^{m+1} \frac{(B^{m+1} + B^m)}{2} + R_D^{m+1}$$

$$+ K_R^{m+1} DO^{(SAT)^{m+1}}. \quad (15)$$

Fig. 1 shows steady-state GEM numerical results compared with steady-state closed form solutions. Both

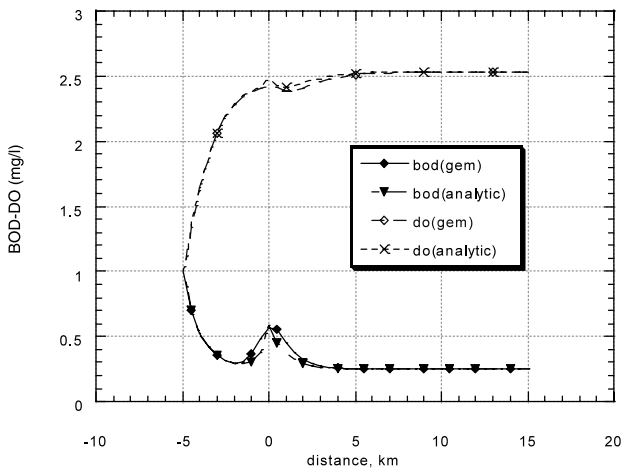


Fig. 1. Comparison of GEM and analytic BOD–DO concentrations.

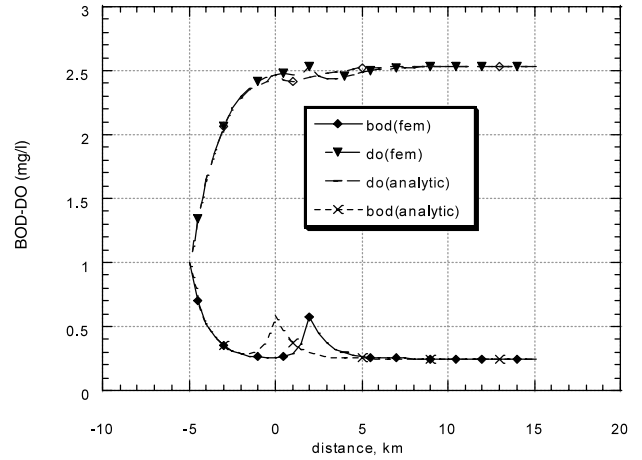


Fig. 2. Comparison of FEM and analytic BOD–DO concentrations.

are very close. We note that GEM has performed excellently in representing point sources. This is primarily due to the second order associated with the boundary integral evaluation of the point source. Particularly suited for point singularities, GEM accurately captures the point load without the need to resort to finer gridding in the vicinity of discharge. As shown in Fig. 2, the same level of accuracy cannot be attributed to the Galerkin’s finite element solutions. Without employing finer grids around the point of discharge, finite element does not yield faithful results. While the profile does not show excellent agreement for the DO distribution in the vicinity of the point load (at  $x = 0$ ), the method also did not perform satisfactorily in modelling point discharge for BOD. The results are not only out of phase at  $x = 0$ , but registers the maximum deviation from the analytical results.

### 5.2. Case 2

This example tests the effects of variable inputs at the upstream boundary. In order to compare the numerical results obtained herein with those in literature, the following problem parameters given by Dresnack and Dobbins [11] are used:  $B(0, t)$  BOD at  $x = 0$  is  $37 + 13 \cos(2\pi t)$  mg/l ( $t = 0$  at noon and it is in hours),  $DO(0, t)$  DO at  $x = 0$  is  $8.5 + 3.5 \cos(2\pi t)$  mg/l,  $E_B = E_D = 4.65 \text{ m}^2/\text{s}$  ( $50 \text{ ft}^2/\text{s}$ ),  $L_B = 5.0 \text{ mg/l/day}$ ,  $K_B = K_D = 0.25/\text{day}$ ,  $K_R = 2.0/\text{day}$ ,  $DO^{SAT} = 9.5 \text{ mg/l}$ ,  $U = 25.7 \text{ km/day}$  (16 miles per day). The analytical solutions for the equilibrium values are given by the authors as  $(BOD)_\infty = L_B / (K_B + K_D) = 10 \text{ ppm}$ , and for  $(DO)_\infty = DO^{SAT} - (K_B / K_R) (BOD)_\infty = 8.25 \text{ mg/l}$ . Their results show that equilibrium results are almost attained at 154.5 km (96 miles) downstream after 144 h of simulation. Figs. 3 and 4 show the numerical GEM and FEM results of BOD and DO computed at the end of

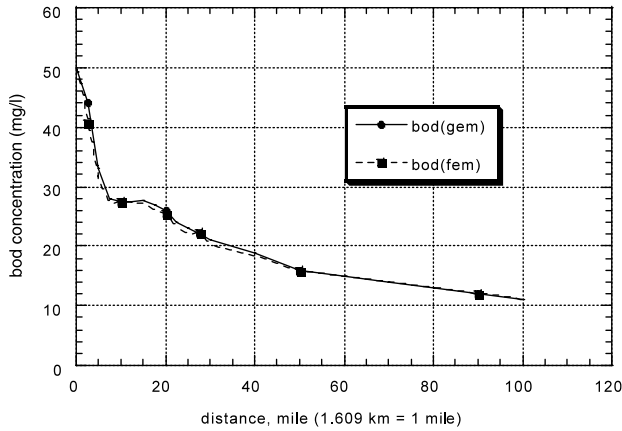


Fig. 3. GEM and FEM numerical results for BOD concentrations after 144 h (harmonic input).

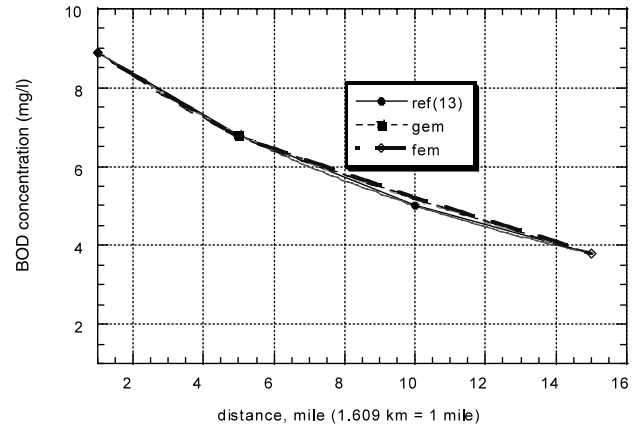


Fig. 6. Comparison of GEM, FEM and published BOD results after 216 h (steady input).

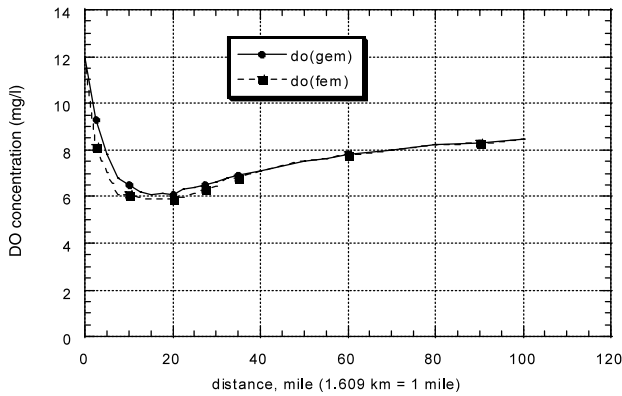


Fig. 4. GEM and FEM numerical results for DO concentrations after 144 h (harmonic input).

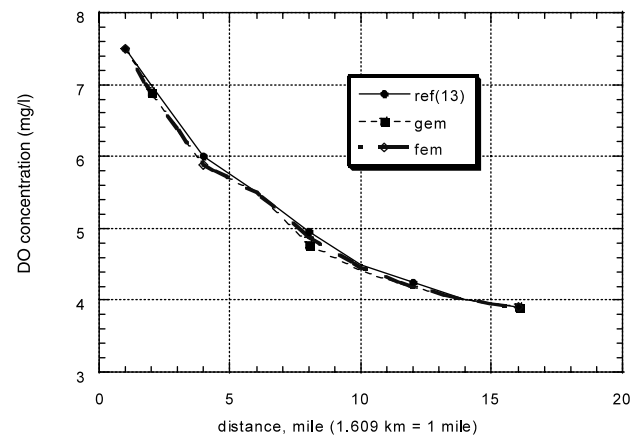


Fig. 7. Comparison of GEM, FEM and published DO results after 216 h (steady input).

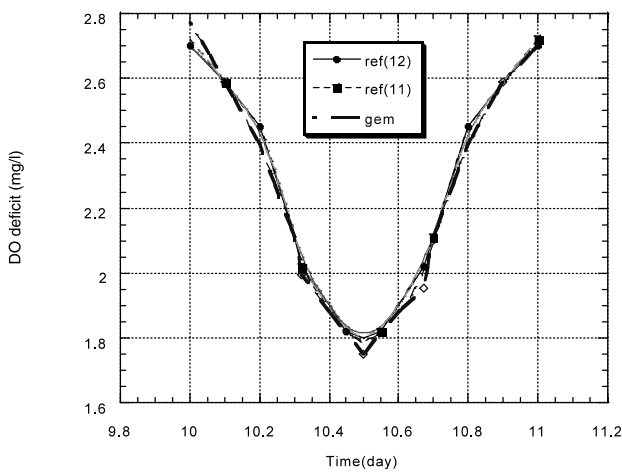


Fig. 5. Comparison of GEM and published results for DO deficit (mg/l).

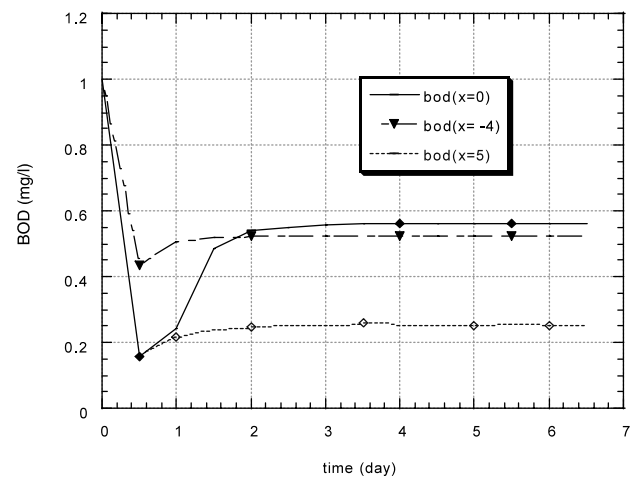


Fig. 8. BOD profiles at different locations.

144 h of simulation as can be seen from these figures, both of them converge to the analytical results given above.

Next, we compare the DO deficit ( $DO^{SAT} - DO$ ) analytical model results of Adrian and Alshawabkeh [12] with the numerical results obtained in this study, and the

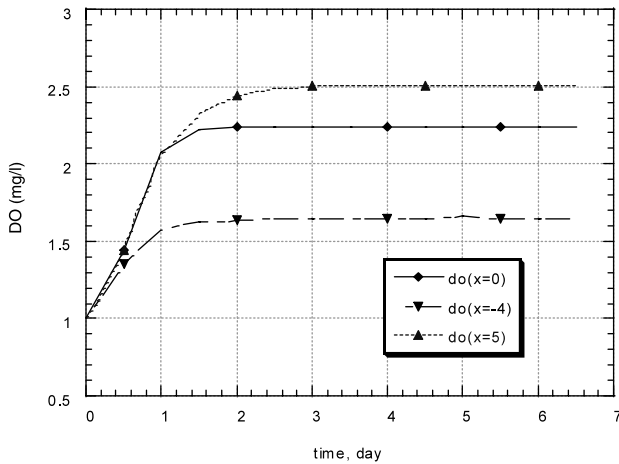


Fig. 9. DO profiles at different locations.

finite difference solutions of Dresnack and Dobbins [11]. The same problem parameters as before are applied. Fig. 5 shows a comparison of different solutions of dissolved oxygen deficit as a function of time. Both FEM and GEM results are indistinguishable, so only those of GEM are plotted. As can be observed, the numerical results compared excellently with analytical.

### 5.3. Case 3

We test the ability of GEM to handle constant inputs of BOD and DO at the upstream boundary. In order to enable us compare numerical and closed form results, the same problem parameters as those of Hann and Young [12] are utilized;  $B(0, t)$  BOD at  $x = 0$  is 8.817 mg/l,  $DO(0, t)$  DO at  $x = 0$  is 7.56 mg/l.  $E_B = E_{DO} = 37.16$  m<sup>2</sup>/s (400 ft<sup>2</sup>/s),  $U = 0.061$  m/s (0.2 fps),  $K_D = 0.23$ /day,  $K_R = 0.1$ /day,  $K_B = 0.0$ ,  $DO^{SAT} = 8.0$  mg/l,  $\Delta x = 0.805$  km (0.5 miles) and  $\Delta t = 0.05$  days. Figs. 6 and 7 show BOD and DO results obtained at the end of 216 h of simulation. All the results agree excellently with the analytical solution given by Hann and Young [13].

### 5.4. Case 4

In order to verify the reliability of GEM in describing the physics of time-dependent point discharge, the magnitude of the point loads given in *Case 1*, are introduced at  $t = 0.1$  days. The effects on the BOD and DO profiles at various sections of the problem domain ( $x = 0$ ,  $x = -4$  km,  $x = 5$  km) are shown in Figs. 8 and 9. The results are well represented from a qualitative point of view. We note that at  $t = 0.1$  days and  $x = 0$ , the impact of the point load is very noticeable. In addition,

the results approach the expected steady state solutions in both cases.

## 6. Conclusion

The reliability of GEM in simulating BOD–DO dynamics in a river has been demonstrated. It has been shown that GEM is capable of handling point discharges because the resulting singularity can be accommodated by its singular integral formulation. In addition it has also been demonstrated, that GEM does keep commitments in dealing with time-dependent point loads. From the examples treated herein, we observe that GEM performed as good as FEM. We, however, reiterate that the whole idea about GEM is not to displace the older and more entrenched domain-based numerical techniques, but to show that with some modifications, the boundary integral method can handle those problems, which may seem intractable or very tasking to solve by relying solely on the classical approach.

## References

- [1] Guymon GL. A finite element solution of the one-dimensional diffusion–convection equation. *Water Resour Res* 1970;6:204–10.
- [2] Price HS, Cavendish JC, Varga RS. Numerical methods of higher-order accuracy for diffusion–convection equations. *Soc Petrol Eng* 1968;293–300.
- [3] Book DL, Boris JP, Hain K. Flux-convected transport II: generalization of the method. *J Comput Phys* 1975;248.
- [4] Tucci CE, Chen YH. Unsteady water quality modelling for river network. *J Water Res Plan Management Div, Proc ASCE*, 1981;107:477.
- [5] Gray WG, Pinder GF. An analysis of numerical solution of transport equation. *Water Resour Res* 1976;12:547–55.
- [6] Taigbenu AE, Liggett JA. An integral solution of the diffusion–advection equation. *Water Resour Res* 1986;22:1237–46.
- [7] Cheng AH-D. Darcy's flow with variable permeability – a boundary integral solution. *Water Resour Res* 1995;20:2241–63.
- [8] Brebbia CA, Skerget P. Diffusion–advection problems using boundary elements. In: *Proceedings of the Fifth International Conference on Finite Elements in Water Resources*, Burlington, VT, USA: Springer; 1984. p. 747–68.
- [9] Taigbenu AE, Onyejekwe OO. Transient 1-D transport equation simulated by a mixed Green element formulation. *Int J Numer Meth Fluids* 1997;25:437–54.
- [10] Onyejekwe OO. Green element description of mass transfer in reacting systems. *Numer Heat Transfer* 1996;B30:483–98.
- [11] Dresnack R, Dobbins WE. Numerical analysis of BOD and DO profiles. *J Sanitary Eng Div, ASCE*, 1968;94:789–807.
- [12] Adrian DD, Alshawabkeh AN. Analytical dissolved oxygen model for sinusoidally varying BOD. *J Hydrol Eng* 1997;2:180–7.
- [13] Hann Jr RW, Young PJ. Mathematical models of water quality parameters for rivers and estuaries. *Tech. Reports No. 45*, Water Resources Institute, Texas A&M University; 1972.